ELSEVIER

Catalysis Today 79–80 (2003) 391–399

CATALYSIS TODAY

www.elsevier.com/locate/cattod

The palladium catalysed hydrogenation of 2-butyne-1,4-diol in a monolith bubble column reactor

J.M. Winterbottom [a,*], H. Marwan [b], E.H. Stitt [c], R. Natividad [a]

[a] *School of Chemical Engineering, The University of Birmingham, Edgbaston, Birmingham B15 2TT, UK*
[b] *Chemical Engineering Department, Syah Kuala University, Banda Aceh 2311, Indonesia*
[c] *Synetix, Belasis Avenue, PO Box, Billingham, Cleveland Ts23 1LB, UK*

Abstract

A monolithic cocurrent downflow contactor (CDC) reactor was used for the palladium catalysed liquid phase hydrogenation of 2-butyne-1,4-diol (B) to *cis*-2-butene-1,4-diol (C) in the temperature range 293–333 K and in the pressure range 102–304 kPa. Its performance was compared with a slurry CDC reactor and a stirred tank reactor (STR). Apparent energy of activation (46–54.5 kJ/mol) and transport calculations indicated the reaction was surface rate controlled. A Langmuir–Hinshelwood mechanism was used to model the reaction. A good agreement was found between the rates from the model and the experimental rates. Selectivity to the product C was significantly greater for the monolith and slurry CDC (0.980–0.993) compared with the STR (0.90–0.95) at conversions of B approaching 100%. It was concluded that the monolith CDC possesses a performance comparable with the slurry CDC particularly in the selective production of C, but has the added advantage of allowing easy catalyst separation.
© 2003 Elsevier Science B.V. All rights reserved.

Keywords: Hydrogenation; 2-Butyne-1,4-diol; Monolith bubble column reactor

1. Introduction

The selective hydrogenation of 2-butyne-1,4-diol (B) to *cis*-2-butene-1,4-diol (C) has been studied for long time since (C) is an important intermediate in the production of endosulfan (insecticide) and Vitamins A and B_6. Scheme 1 depicts the possible products obtained by the hydrogenation of B [1,2].

Various studies regarding the selective hydrogenation of B to C over palladium catalysts have been usually performed in stirred reactors [3–6] and include kinetic and selectivity studies. Modelling has been based on a dual-site Langmuir–Hinshelwood mechanism usually with evidence of significant inhibition by the alkyne (B) [4,6], along with a significant range of selectivities to the olefin (C), even with palladium. Scale-up in stirred tank reactors (STRs) from bench-scale to industrial scale, while theoretically possible is practically unattainable because power requirements rule out high stirring speeds, leading to increased mass transport resistances.

Intensified mass transfer can be achieved by use of eductor type systems. One such device is the cocurrent downflow contactor (CDC) reactor [7–9]. The CDC exploits a simple orifice based eductor to create a dense, stable gas–liquid dispersion. It has been reported [7–9] that the CDC, either in slurry or fixed bed mode, is a device that can be operated with high gas-hold-up (0.4–0.5) and high mass transfer effi-

* Corresponding author. Tel.: +44-121-414-5293; fax: +44-121-414-5324.
E-mail address: j.m.winterbottom@bham.ac.uk (J.M. Winterbottom).

0920-5861/03/$ – see front matter © 2003 Elsevier Science B.V. All rights reserved.
doi:10.1016/S0920-5861(03)00069-5

Nomenclature

a_p	external particle area (m^2)
A_1	mass transfer area form gas plug to wall via film (m^2)
A_2	mass transfer area form liquid plug to wall (m^2)
A_3	mass transfer area form gas plug to liquid plug (m^2)
B	2-butyne-1,4-diol
C	2-butene-1,4-diol
Ca	capillary number $= U_b\mu_L/\sigma$
C_B	2-butyne-1,4-diol concentration
C_{H_2}	bulk liquid phase hydrogen concentration (kmol/m^3)
$C_{H_2,S}$	surface concentration of hydrogen (kmol/m^3)
$C^*_{H_2}$	equilibrium liquid phase hydrogen concentration (kmol/m^3)
d_h	cross-sectional channel area/wetted perimeter (m)
d_p	particle diameter
D_{H_2}	diffusion coefficient for H_2 (m^2/s)
F_L	liquid flow-rate (m^3/s)
g_{cat}	mass catalyst (g or kg)
k	overall rate constant
k_r	reaction rate constant $((m^3)^2/(kmol\,kg_{Pd}\,s))$
k_{SL}	liquid–solid mass transfer coefficient
k_1	mass transfer coefficient (gas to wall via film) (m/s)
k_2	liquid–solid mass transfer coefficient (liquid plug to wall) (m/s)
K_H, K_B	adsorption coefficients respectively for H_2 and B (m^3/kmol)
N	molar flux (kmol/(m^2 s))
Re_p, Re_L	particle, liquid Reynolds number
R_1	reaction rate for 2-butyne-1,4-diol hydrogenation (kmol H_2/(m^3 s))
S	selectivity to 2-butene-1,4-diol
Sc	Schmidt number $= \mu_l/\rho_l D_{H_2}$
Sh	Sherwood number
U_b	bubble velocity in monolith channel (m/s)
U_{ls}	liquid velocity in monolith channel (m/s)
W	velocity ratio for fraction of liquid deposited on walls $= (U_b - v_{ls})/U_b = 0.05$
X_{LS}	% liquid–solid transport resistance

Greek letters

δ_f	film thickness (m)
μ_L	liquid viscosity (kg/(m s))
σ	surface tension (N/m)

ciency that can give negligible transport resistances (<4%) with improved selectivity and is process intensive [10].

Honeycomb monoliths are structures consisting of straight and uniform channels that can serve as catalyst support in fixed bed reactors. Monolith catalysts were confined for a long time to application in gas–solid processes, mainly to the area of exhaust gas purification. Since the introduction of the monolith multiphase reactor several investigations have been accomplished in order to increase the utilisation of monolithic structures as catalyst support in multiphase reactions, mainly in processes like hydrogenation and oxidation. Although these catalysts have been shown to possess distinct advantages due to low pressure drop, easy scale-up and improved mass transfer resistance [11,12], their use is not widespread. This paper presents comparable data for CDC operation in slurry, fixed bed and monolith mode as well as a STR. It demonstrates that the monolith CDC reactor is an advantageous alternative to the slurry CDC reactor and STR.

2. Experimental methods

2.1. Equipment

(a) CDC reactor: the operation and schematic reactor diagrams have been reported elsewhere [9], but Fig. 1 shows the schematic of the CDC reactors. The total volume of the system was 0.01 m^3. Liquid flow-rates were in the range 0.50–1.00 × 10^{-4} m^3/s (slurry CDC) and 1.00–1.50 × 10^{-4} m^3/s (monolith CDC). The reactors could be operated in the temperature range 293–333 K and

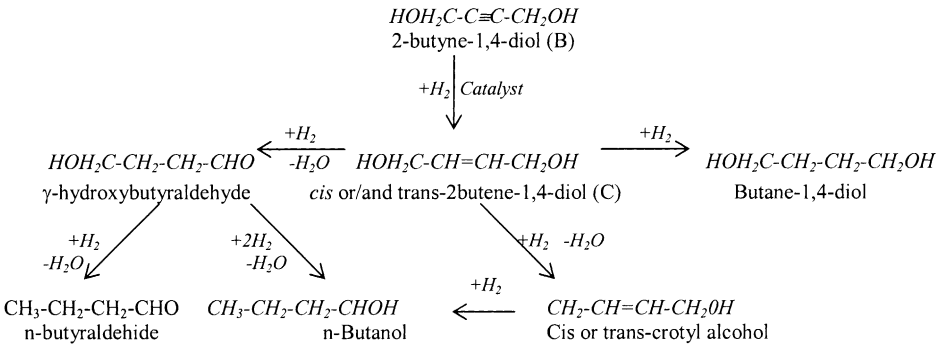

Scheme 1. Reaction network for 2-butyne-1,4-diol hydrogenation.

in the pressure range 152–304 kPa. Hydrogen was supplied via a hydrogen control unit connected to a chart recorder, which monitored and recorded the consumption of hydrogen with time. From the resulting data graph it was possible to determine the slope of the hydrogen consumption plot during the initial 10% conversion of 2-butyne-1,4-diol. The hydrogen was supplied at a rate sufficient to keep a constant dispersion height in the case of monolith and slurry CDC reactors and to maintain the operating pressure in the STR at a set value.

(b) Stirred tank reactors: atmospheric pressure studies were carried out in a STR of volume 0.5×10^{-3} m^3 liquid capacity, fitted with four baffles and a single stage six blade turbine impeller. Higher pressure studies were performed in a Baskerville 0.5×10^{-3} m^3 autoclave, fitted with a magnetically driven stirrer comprising four 45° pitch blades and four baffles. Hydrogen supply and control was similar to that for the CDC reactors. These were operated in the temperature range 288–333 K with stirring speeds in the range 0–1400 rpm.

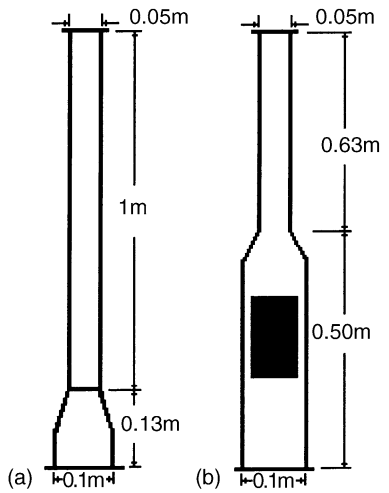

Fig. 1. CDC reactors: (a) Slurry; (b) monolith.

2.2. Catalysts

(a) Pd/monolith catalyst: the catalyst was prepared by impregnation of an α-Al_2O_3 wash-coated cordierite monolith (Johnson–Matthey plc) using sodium tetracholoropallalite solution. The main properties are given in Table 1. After impregnation and drying, the monolith was calcined at 573 K for 12 h and after cooling was installed and reduced in H_2O in the reactor, using hydrogen.

(b) Pd/charcoal powder catalyst (5% (w/w) Pd nominal): the catalyst was a Johnson–Matthey plc Pd/

Table 1
Characteristics of the Pd–monolith catalyst

Property	Parameter value
Pd content (%, w/w)	0.35 (1 wt.% wash-coat)
Wash-coat (%, w/w)	36
Mass Pd/monolith (kg)	2.2068×10^{-3}
Bed length (m)	15.24×10^{-2}
Bed diameter (m)	9.3×10^{-2}
Cell density (cells/m^2)	62×10^4
Wall thickness (m)	0.018×10^{-2}
Voidage	0.7
External area (m^2 m^{-3})	2690
Pore diameter (m)	3.2×10^{-6}

Table 2
Pd/C-Type 37 characteristics

Metal content (%, w/w)	Metal area (m^2/kg)	Mean particle size (μm)	Density (kg/m^3)	External surface area (m^2/kg)
4.89	1.39×10^4	19	2.15×10^3	150

C-Type 37 with the characteristics given in Table 2 and with metal deposited on the exterior surface.

2.3. Product analysis

Product analysis was carried out by gas chromatography using a Cambridge-Ai-Model 94 instrument, fitted with a FID detector and a 30 m × 0.25 mm id DB-wax column.

2.4. Reaction solvents

In the CDC glass reactors employed, to use water with small bubbles required a high inlet velocity, low column velocity and unacceptable working pressure (>304 kPa), which was unsafe; water can be used in equipment capable of safe operation at pressures >406 kPa. Reaction solvents were H_2O and for the monolithic reactor a binary solvent comprising 30% (v/v) 2PrOH in H_2O (M) was used, giving a bubble size of 3.0 mm, and similar selectivity to water.

2.5. Residence time distribution (RTD)

Under reaction conditions, liquid RTD was determined by injecting a pulse of tracer solution (KCl) into the monolith CDC reactor and conductivity profile was obtained by a probe and data acquisition system. Injection and detection points were respectively 1 cm above and below the monolith block. The conductivity profile was linearly correlated to KCl concentration and liquid RTD was obtained. The injection system was similar to that described in earlier works [10] while the monolith CDC used was described in Section 2.1.

3. Results and discussion

3.1. Hydrodynamics and mass transport

Previous studies of Taylor flow [13–15] and mass transfer of H_2 in a monolith channel indicated that the latter can be described by the following:

(a) Gas to wall via liquid film:

$$N_1 A_1 = k_1 A_1 (C^*_{H_2} - C_{H_2,S}) \quad (1)$$

(b) Liquid plug to wall:

$$N_2 A_2 = k_2 A_2 (C_{H_2} - C_{H_2,S}) \quad (2)$$

(c) Gas plug to liquid plug:

$$N_3 A_3 = k_3 A_3 (C^*_{H_2} - C_{H_2,S}) \quad (3)$$

At steady state if the transfer rate from gas plug to liquid plug is the same as the liquid plug to wall, then

$$NA_T = \left[k_1 A_1 + \frac{k_2 A_2 k_3 A_3}{k_2 A_2 + k_3 A_3} \right] (C^*_{H_2} - C_{H_2,S}) \quad (4)$$

If gas–liquid mass transfer is only 12% of liquid plug to wall [13], then

$$R_1 = NA_T = (k_1 A_1 + 0.107 k_2 A_2)(C^*_{H_2} - C_{H_2,S}) \quad (5)$$

where the mass transfer coefficients are given by

$$k_1 = \frac{D_{H_2}}{\delta_f} \quad (6)$$

and

$$k_2 = \frac{Sh D_{H_2}}{d_h} \quad (7)$$

and other relevant parameters were calculated via the following:

$$Sh = 1.5 \times 10^{-7} Re^{1.648} Sc^{0.177} \left(\frac{\delta_f}{d_h} \right)^{-2.338} \quad (8)$$

$$\delta_f = 0.18 d_h \lfloor 1 - \exp(-31 Ca^{0.54}) \rfloor \quad (9)$$

Finally, the surface concentration of hydrogen from Eq. (5) was used to estimate the diffusional resistance:

$$X_{LS} = \frac{C^*_{H_2} - C_{H_2,S}}{C^*_{H_2}} \times 100 \quad (10)$$

Table 3 shows the transport parameters assuming Taylor flow for the monolith block for which the reaction rate units are not identical to those in Table 4.

Table 3
Transport parameters for the Pd–monolith catalyst[a]

Temperature (°C)	R_1 (kmol H_2/(m^3 s))	$C^*_{H_2}$ (kmol/m^3)	k_1 (m/s)	k_2 (m/s)	$C_{H_2,S}$ (kmol/m^3)	X_{LS} (%)
35	5.1×10^{-5}	2.67×10^{-3}	3.14×10^{-4}	9×10^{-7}	2.46×10^{-3}	8.0
45	8.98×10^{-5}	2.66×10^{-3}	4.19×10^{-4}	1.6×10^{-7}	2.38×10^{-3}	10.0
55	1.24×10^{-4}	2.62×10^{-3}	5.66×10^{-4}	3.1×10^{-7}	2.33×10^{-3}	11.0

[a] $P = 304$ kPa; solvent = M; $\sigma = 47.2 \times 10^{-3}$ N/m; $U_{ls} = 0.0162$ m/s; $U_b = 0.0171$ m/s; $d_h = 0.00055$ m; $A_1 = 1.67\,m^2$; $A_2 = 1.11\,m^2$.

Table 4
Mass transport characteristics for slurry CDC reactor ($T = 35$ °C)

Pressure (kPa)	Solvent	R_1 (kmol H_2/(m^3 s))	k_{SL} (m/s)	$C^*_{H_2}$ (kmol/m^3)	$C_{H_2,S}$ (kmol/m^3)	X_{LS} (%)
203	H_2O	7.5×10^{-6}	4.5×10^{-2}	1.304×10^{-3}	1.293×10^{-3}	0.89
304	M	4.1×10^{-5}	0.00918	2.67×10^{-3}	2.65×10^{-3}	0.76

Liquid–solid mass transfer coefficients (k_{SL}) were also calculated for slurry CDC reactors using suitable forms of the Frössling equation as follows:

$$Sh = \frac{k_{SL} d_p}{D_{H_2}} = 2 + 3.98\, Re_p^{1/4} Sc^{1/3} \quad (Re_p > 10\,000) \tag{11}$$

$$Sh = 2 + 0.089\, Re_p^{2/3} Sc^{1/3} \quad (Re_p < 10\,000) \tag{12}$$

Liquid properties were employed to calculate Re_p for reasons explained elsewhere [8–10]; a mean k_{SL} was used for the whole reactor. A detailed explanation can be found in [9]. Transport parameters found for slurry CDC reactor are listed in Table 4.

As observed in earlier studies [9], the X_{LS} value for the slurry CDC reactor is very small (<1%). The monolithic CDC reactor compares favourably with the slurry CDC reactor and this is supported by apparent energy of activation values which were 55.3±1 kJ/mol (slurry CDC) and 47.3 ± 1 kJ/mol (monolith CDC), both indicating surface reaction rate control.

3.2. Kinetics

The effect of hydrogen partial pressure on initial reaction rates was studied in the monolithic CDC in the hydrogen partial pressure range of 0–355 kPa at a temperature of 308 ± 1 K. A linear relationship with positive slope was observed suggesting the reaction to be first order with respect to hydrogen partial pressure. Analogous measurements made for slurry CDC and STR resulted in a similar observation.

The effect of initial B concentration on the initial rate (R_1) was investigated at 308 K and 305 kPa in the three reactors. It was found that in the slurry CDC and STR the reaction rate decreased with increase in B concentration indicating a substrate inhibited kinetics, while the opposite trend occurred in the monolithic CDC reactor. Such differences can be inferred from the reaction order (m) with respect to B, being m determined by means of a convenient graphical procedure (Fig. 2).

It is interesting to observe (Table 5) that the reaction rate only in the monolith CDC reactor is

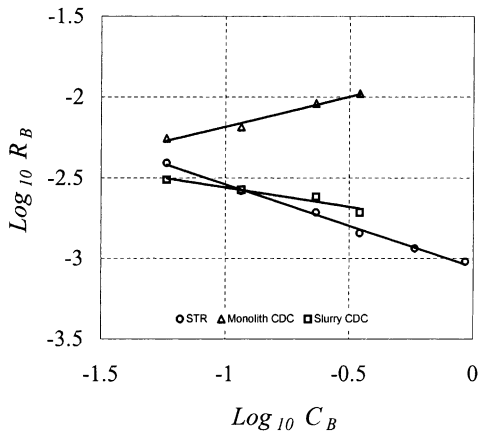

Fig. 2. Determination of selective hydrogenation of B to C reaction order with respect to B.

Table 5
Power law rate expressions for 2-butyne-1,4-diol hydrogenation[a]

Reactor	Rate expression
Monolith CDC	$R_1 = wkC_{H_2}^{1.0}C_B^{0.37}$
Slurry CDC	$R_1 = wkC_{H_2}^{1.0}C_B^{-0.24}$
STR	$R_1 = wkC_{H_2}^{1.0}C_B^{-0.52}$

[a] $T = 35\,^{\circ}C$; $P_{H_2} = 0$–$304\,kPa$ (monolith CDC), $P_{H_2} = 0$–$304\,kPa$ (slurry CDC), $P_{H_2} = 101$–$608\,kPa$ (STR).

related by a positive order with the variation of 2-butyne-1,4-diol concentration. Even in the literature the only non-negative order reported was zero [16] in a reaction using Raney nickel catalyst which is less active compared with palladium.

3.2.1. Kinetic model

The hydrogenation of B is relatively slow and at the temperature at which kinetics were measured (308 K), the apparent energy of activation lay in the range of 46–54.5 kJ/mol, which is what may be expected for a surface reaction rate controlled hydrogenation of an alkyne. Also, transport calculations (Tables 3 and 4) indicated that the surface concentration of hydrogen was almost the same as that in the bulk solution, again indicating that the reaction was surface reaction rate controlled and that the mass transfer limitations can be eliminated. Considering the above, the reaction was analysed for the three reactors based upon a dual-site Langmuir–Hinshelwood (L–H) mechanism, giving a rate equation of the form:

$$R_1 = \frac{k_r C_{H_2,S} C_{B,S}}{(1 + K_H C_{H_2,S} + K_B C_{B,S})^2} \quad (13)$$

The above does not necessarily imply that a Rideal–Ely mechanism occurs (i.e. reaction via non-adsorbed dihydrogen). The simultaneous (addition of two atoms of adsorbed hydrogen) or the sequential (addition of two atoms of hydrogen) to B and to its half-hydrogenated state would give the same mathematical result. Hence the above represents a "lumped parameter" approach and in any case, other models gave negative values of K_H and K_B parameters on calculation. The parameters k_r, K_H and K_B were estimated via a non-linear least squares regression analysis, for which the sum of squares (SSR) of the difference between the observed and predicted rates was minimised by the Marquardt method [17] for each reactor. The estimated parameters are shown in Table 6 with their corresponding confidence interval calculated considering a confidence level of 95%. These parameters gave good agreement for the rates from the L–H and the experimental rates (Fig. 3). It can be observed that the confidence interval for the parameter K_H mainly for the monolith CDC, is large compared with its actual value. Precise parameter estimation would have required that the experimental variables, i.e., $C_{H_2,S}$ and $C_{B,S}$ were varied simultaneously. Although the mathematical model generates values of k_f, K_H and K_B, the parameters in the L–H model are products of K_H, K_B, C_H and C_B, so that the variation of K_H and K_B as a function of reactor environment may be apparent, because there is no means of knowing $C_{H_2,S}$ and $C_{B,S}$ precisely and the real influential parameters are the products $K_H C_{H_2,S}$ and $K_B C_{B,S}$. It is also obvious that K_H and K_B will be constant at a given temperature, since they are equilibrium constants and should not vary from one reactor to another, but the surface populations (θ_H and θ_B) will be a function of K_H, K_B, C_{H_2} and C_B. C_{H_2} and C_B could vary even though transport limitation is negligible and also, therefore, θ_H and θ_B.

In this case, although $C_{H_2,S}$ and $C_{B,S}$ are assumed to be the same as their bulk solution values, if the characteristics of the reactor are such that hydrogen availability on the surface is enhanced then $C_{H_2,S}/C_{B,S}$ may increase, thus increasing the fractional surface coverage of hydrogen (θ_H). The ratio of surface coverage θ_H/θ_B will be given by $K_H C_{H_2,S}/K_B C_{B,S}$, so that if the reactor/catalyst combination gives rise to dif-

Table 6
Kinetic parameters derived from non-linear least squares regression

Reactor	$C^*_{H_2} \times 10^4$ (kmol/m^3)	k_r ((m^3)^2/(kmol kg$_{Pd}$ s))	K_H (m^3/kmol)	K_B (m^3/kmol)	SSR (kmol/(kg$_{Pd}$ s))
Monolith	26.73	$0.3061 \pm 4 \times 10^{-4}$	0.5631 ± 0.2848	$2.58 \pm 1.9 \times 10^{-3}$	9.97×10^{-11}
Slurry	20.65	245.66 ± 0.72	3.36 ± 0.72	$12.49 \pm 1.8 \times 10^{-2}$	1.17×10^{-6}
STR	6.5	114.53 ± 0.07	2.69 ± 0.45	$27.66 \pm 9.6 \times 10^{-3}$	4.74×10^{-9}

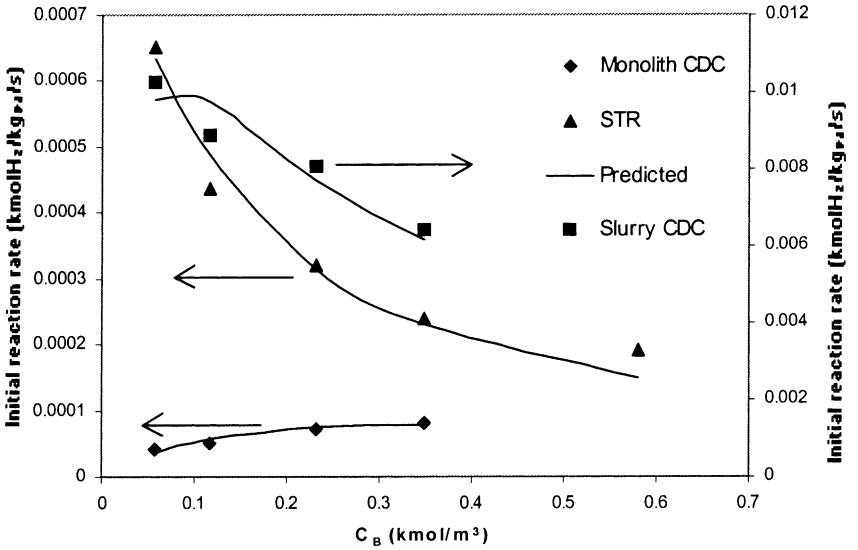

Fig. 3. Rate vs. 2-butyne-1,4-diol concentration in monolith CDC, slurry CDC and STR reactor.

ferent θ_H/θ_B values, then kinetics can vary. This type of effect was reported previously [18,19] for a STR and slurry CDC reactor respectively and by Moulijn [20], who attributed such observed effects to modified surface concentration. These effects can therefore occur and are not a function transport effects. It is well known that heterogeneous reactions can change order over a concentration range of a specific reactant (A) due to changes in fractional surface occupation (θ) of A, so that depending upon the bulk concentration of a specie the order can change from one (low concentration) to zero (high concentration) to and, of course at high concentrations, there is the possibility of negative orders due to very strong adsorption.

The slurry CDC has a kinetic performance lying between the monolith CDC and STR reactors, but it is a very efficient mass transfer device (Table 4) and it has been reported elsewhere that Pd/C catalysts may give rise to enhanced mass transfer coefficients (k_{SL}) due to carbon particles adhering to the gas bubble–liquid interface [8,21] in a very turbulent regime, particularly at the inlet. This will result in shorter diffusion paths and enhancement of hydrogen concentration at the catalyst surface.

It was also observed that while the apparent activation energy in the STR was 46–50 kJ/mol at the lower temperatures (293–308 K), it decreased to 33–38 kJ/mol at higher temperatures (308–338 K) indicating the presence of more significant diffusional control in the STR when the hydrogenation rate of B increased significantly. Furthermore, the use of a fixed bed CDC reactor give rise to relatively low apparent activation energy values in the range 25–46 kJ/mol, depending on the intensity of gas–liquid-catalyst contact [22].

The above (L–H) model also allowed quite a reasonable prediction of product distribution (Fig. 4). This was obtained by solving numerically (Runge Kutta 4th order method) the following equations

$$-\frac{dB}{dt} = \frac{k_r K_H K_B C_{H_2,S} C_B}{(1 + K_H C_{H_2,S} + K_B C_B)^2} \quad (14)$$

$$\frac{dC}{dt} = \frac{k_r K_H K_B C_{H_2,S} C_B}{(1 + K_H C_{H_2,S} + K_B C_B)^2} \quad (15)$$

3.2.2. Selectivity measurements

Selectivity (S) to C was very high, both in the case of the slurry CDC and monolith CDC reactor was in the range 0.980–0.993 at conversion of B approaching 100%. The STR gave selectivities in the range 0.90–0.95. Selectivity values are shown in Table 7.

3.2.3. RTD studies

Monolith and slurry CDC reactors have an element of plug flow characteristic and this has been reported for the slurry CDC reactor [23]. In the case of the

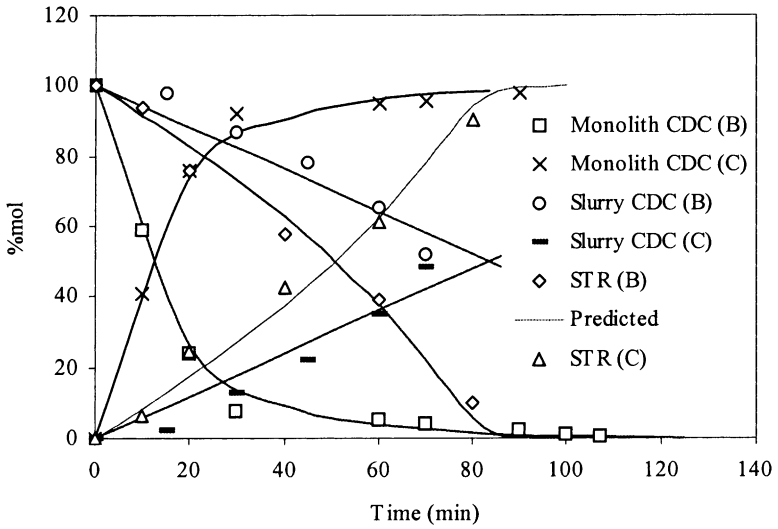

Fig. 4. Product distribution for different reactors.

Table 7
Selectivity (S) for hydrogenation of B to C[a]

Reactor	w (kg/m^3)	Solvent	Selectivity (S) to C at 95% conversion of B
Monolith	2.2068/bed	M	0.979
Slurry	0.1	M	0.975
		H_2O	0.960
STR	4	H_2O	0.9000

[a] T = 35 °C; C_B = 0.23 kmol/m^3; M = 30% (v/v) 2ProH–H_2O.

monolith CDC reactor, Taylor flow of gas and liquid was assumed and later confirmed [24] and RTD measurements indicated laminar flow, with a stagnant wall film suggested by the tail of the distribution curve

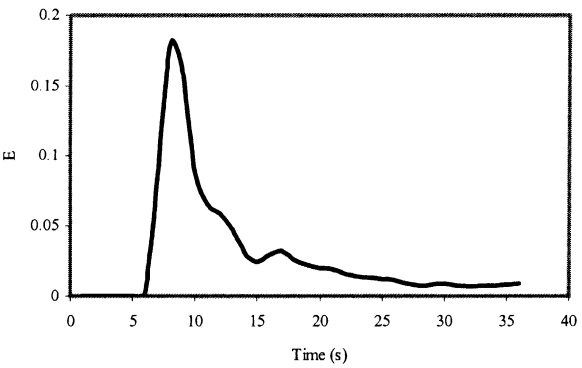

Fig. 5. RTD for monolith CDC.

(Fig. 5). The reaction rate per unit volume of reactor was greater for the monolith CDC reactor and selectivity to the product C was significantly greater for the monolith and slurry CDC reactors compared with the STR, probably because the former reactors possessed some plug flow characteristics, while STR is well mixed. However, until a precise knowledge of the hydrodynamics is available, the effect of dispersion cannot be included in product distribution modelling.

4. Conclusions

It is concluded that the monolith CDC reactor possesses some very distinct and promising advantages compared with the other reactor forms, with low transport resistances and no catalyst separation problems. Concentration profiles may be quite complex along the channels and significantly different kinetic performance was observed. A monolith CDC is comparable with the slurry CDC reactor particularly in the selective production of C.

Acknowledgements

The authors H. Marwan and R. Natividad are grateful to Indonesian government and CONACYT (Mexico) respectively for financial support. Thanks are also

extended to ICI Synetix, Johnson–Matthey plc and Norton Chemical for provision of catalysts.

References

[1] J.M. Winterbottom, H. Marwan, J. Valadevall, S. Sharma, S. Raymahasay, Heterogeneous catalysis and fine chemicals IV, in: H.V. Blaser, A. Baiker, R. Prins (Eds.), Stud. Surf. Sci. Catal. 108 (1997) 59.
[2] T. Fukuda, T. Kusama, Bull. Chem. Soc. Jpn. 20 (1958) 28.
[3] R.V. Chaudhari, M.G. Parande, P.A. Ramachandran, H.G. Vadgaonkar, R. Jaganathan, AIChE J. 31 (1985) 1891.
[4] R.V. Chaudhari, R. Jaganathan, D.S. Kolhe, G. Emig, H. Hofmann, Appl. Catal. 29 (1978) 141.
[5] T.W. Russel, D.M. Duncan, J. Org. Chem. 39 (1974) 3050.
[6] A.N. Gryaznor, T.M. Blosljudova, A. Maganjuk, A.N. Karanov, A.V. Ermolaev, I.K. Sarajcheva, UK Patent No. 2 096 595a (1982).
[7] X. Lu, A.P. Boyes, J.M. Winterbottom, Chem. Eng. Sci. 49 (1994) 5719.
[8] J.M. Winterbottom, Z. Khan, A.P. Boyes, S. Raymahasay, Catal. Today 48 (1999) 221–228.
[9] J.M. Winterbottom, Z. Khan, S. Raymahasay, G. Knight, N. Roukounakis, J. Chem. Tech. Biotechnol. 75 (2000) 1015.
[10] H. Marwan, S. Raymahasay, J.M. Winterbottom, in: Proceedings of the Second International Conference on Process Intensification in Practice, Antwerp, October 1998, J. Semel. Ed. Lond. 109–124.
[11] B. Andersson, S. Irandoust, A. Cybulski, in: A. Cybulski, J.A. Moulijn (Eds.), Structured Catalysts and Reactors, Marcel Dekker, New York, 1998, Chapter 10, pp. 267–303. ISBN 0-8247-9921.6.
[12] F. Kapteijn, J.J. Heiszwolf, T.A. Nijhuis, J.A. Moulijn, Cat-tech 3 (1999) 24.
[13] V. Hatziantoniou, B. Andersson, H.H. Schoon, Ind. Eng. Chem. Proc. Des. Dev. 25 (1986) 964.
[14] S. Irandoust, B. Andersson, Chem. Eng. Sci. 43 (1988) 1983.
[15] T.C. Thulasidas, M.A. Abraham, R.L. Cerro, Chem. Eng. Sci. 5 (1995) 183.
[16] C. Rongfu, G. Qiwei, J. East Chin. Inst. Chem. Tech. 14 (1988) 269.
[17] D. Marquardt, SIAM J. 11 (1963) 431.
[18] G.J.K. Acres, B.J. Cooper, J. Appl. Chem. Biotechnol. 22 (1972) 769.
[19] Z. Khan, Ph.D. Thesis, University of Birmingham, 1995.
[20] J.A. Moulijn, in: J.A. Moulijn, P.W.M.N. van Leeuwen, R.A. van Santen (Eds.), Catalysis: An Integrated Approach to Homogeneous, Heterogeneous and Industrial Catalysis, Elsevier, Amsterdam, 1993, Chapter 3, pp. 73–78.
[21] M. van der Zon, P.J. Hamersma, E.K. Poels, A. Bliek, Catal. Today 48 (1999) 131–138.
[22] H. Marwan, Ph.D. Thesis, University of Birmingham, 1998, p. 280.
[23] A.P. Boyes, A. Chugtai, Z. Khan, S. Raymahasay, A.T. Sulidis, J.M. Winterbottom, J. Chem. Tech. Biotechnol. 64 (1995) 55–65.
[24] M.D. Mantle, A.J. Sederman, S. Raymahasay, E.H. Stitt, J.M. Winterbottom, L.F. Gladden, AIChE J. 48 (2002) 909–912.